

## ANALYTICAL DISCRETE STACKING SEQUENCE OPTIMIZATION OF RECTANGULAR COMPOSITE PLATES SUBJECTED TO BUCKLING AND FPF CONSTRAINTS

ALEKSANDER MUC, MAŁGORZATA CHWAŁ

*Cracow University of Technology, Kraków, Poland*

*e-mail: olekmuc@mech.pk.edu.pl; mchwal@pk.edu.pl*

A special type of new discrete design variables is introduced in order to find optimal stacking sequences for laminated structures. Using the proposed new design variables, we demonstrate how to find analytical (i.e. without any numerical optimization algorithm) optimal solutions for laminates made of plies having three different fibre orientations:  $0^\circ$ ,  $\pm 45^\circ$ ,  $90^\circ$ . It is proved that the definition of design variables enables us to distinguish two types of optimal solutions, i.e. unimodal and bimodal ones. The form of optimal stacking sequences affects the multiplicity (bimodal problems) or uniqueness (unimodal problems) of the solutions. The decoding procedure between membrane and flexural design variables is also proposed. The results demonstrate the effectiveness, simplicity and advantages of the use of design variables, especially in the sense of the accuracy, repeatability of results and convergence of the method.

*Keywords:* stacking sequence optimization, composite plates, buckling, first-ply-failure

### 1. Introduction

The superior mechanical properties of composite materials such as high stiffness, weight ratio and anisotropic properties that can be tailored through variation of fiber orientations and stacking sequence give the designer an added degree of flexibility. However, this additional tool should be used by engineers in a proper manner, i.e. it requires an application of optimization methods. For many design problems using the 2D approach (beams, plates, shells), most notably for those where stiffness requires domination, there are multiple designs with similar performance. These designs may have very different stacking sequences but very similar or almost identical values of stiffnesses  $\mathbf{A}$  and  $\mathbf{D}$ . In such cases, it is important to produce all or most of the design alternatives.

The effectiveness of optimal design, especially for composite structures, is strongly dependent on the proper choice of two elements: i) definition of design variables, ii) application of an appropriate optimization algorithm.

The simplest definition of design variables depends on direct application of real continuous variables (i.e. fibre orientations  $\theta_l$  and thicknesses  $t_l$  in the  $l$ -th ply,  $l = 1, 2, \dots, N$ ). Now, such an approach is commonly used in finite element codes, such as e.g. ANSYS, ABAQUS etc. This method is not very convenient for many engineering or analytical applications and is replaced by the introduction of so-called lamination parameters (Miki, 1986; Fukunaga and Vanderplaats, 1991). The lamination parameters are usually determined for thin walled composite structures (i.e. beams, plates or shells) with the use of the Love-Kirchhoff kinematical hypothesis. For an arbitrary laminate, the structural stiffness is characterized by 12 independent parameters instead of  $2 \times N - 1$  variables for the previous real continuous variables ( $\theta_i$  and  $t_i$ ). In fact, analytical

studies deal mainly with the use of four of them, i.e.  $\xi_{[1]}^{\{A\}}$ ,  $\xi_{[2]}^{\{A\}}$ ,  $\xi_{[1]}^{\{D\}}$ ,  $\xi_{[2]}^{\{D\}}$  corresponding to laminates in which the stiffnesses  $B_{ij}$ ,  $A_{16}$ ,  $A_{26}$ ,  $D_{16}$  and  $D_{26}$  are assumed to be equal to zero.

The past few decades have seen an increased interest in general-purpose “black-box” optimization algorithms that exploit limited knowledge concerning the optimization problem on which they are run. In particular, the two most popular black-box optimization strategies, evolutionary algorithms and simulated annealing, mimic processes in natural selection and statistical mechanics, respectively. Commonly, they are based on the standard use of the lamination parameters. In this case it is impossible to find a unique laminate configuration, and, in addition, the correctness and accuracy of solutions can be verified by the comparison with other numerical result only.

According to the definitions and classifications of IEEE NNC (1996) the four types of algorithms constitute evolutionary computation methods (Genetic Algorithms – GA, Evolutionary Programming – EP, Evolution Strategies – ES and Genetic Programming – GP) but in general they are based on the Darwinian concept of evolution. In fact, now hybrids of the four methodologies are becoming most popular. The distinguishing feature of traditional Darwinistic evolution is selection, the survival of the fittest members of each generation. For composite materials it is much better to look beyond that view in the sense of the above algorithms and to explore a new view of evolution that includes natural selection plus self-organization – see Kauffmann (1993). It is worth to emphasize that Grosset *et al.* (2006) formulated almost the same conclusions and stated that it was necessary to abandon partially the Darwinistic theory of evolution and finally introduced to the analysis of composites the concept of estimation of distribution algorithms. They used a statistical framework to formalize the search mechanisms.

However, it has become important to understand the relationship between how well an algorithm performs and the optimization problem on which it is run. In this paper, we present an analysis that contributes toward such an understanding by addressing questions like the following: how we can best match design variables and algorithms to the problems, i.e., how best we can relax the black-box nature of lamination parameters and the algorithms and have them exploit some knowledge concerning the optimization problem?

In the present paper, we intend to solve the problem of optimal design of bi-axially compressed rectangular multilayered composite plates having discrete fibre orientations in each individual ply and subjected to buckling and FPF constraints. Contrary to the identical problems discussed in the literature, we look deeper into the physical problem considered herein. We demonstrate that the appropriate definition of design variables allow us to obtain unique, exact and accurate solutions. Using the proposed new design variables we show how to find analytical (i.e. without any numerical optimization algorithm) optimal solutions for laminates made of plies having three different fibre orientations:  $0^\circ$ ,  $\pm 45^\circ$ ,  $90^\circ$ . For a higher number of different discrete fibre orientations, we propose the application of an effective numerical algorithm based on the evolution strategy, see Muc and Muc-Wierzgoń (2012). We explain also the discussed in the literature problem of multiplicity of optimal solutions. We prove that the multiplicity is an artificial result since it is caused by wrong coding of laminate configurations and wrong interpretation of optimal solutions.

The numerical results, presented in the paper, are obtained for a graphite/epoxy resin material having the following mechanical properties:  $E_1 = 127.59$  GPa,  $E_2 = 13.03$  GPa,  $G_{12} = 6.41$  GPa,  $\nu_{12} = 0.3$ , and the thickness of an individual ply in the laminate is equal to 1.27 mm. The ultimate allowable strains are following:  $\varepsilon_{1allowable}^{local} = 0.008$ ,  $\varepsilon_{2allowable}^{local} = 0.029$ ,  $\gamma_{12allowable}^{local} = 0.015$ . A safety factor equal to 1.5 is used to calculate the strain allowables.

## 2. Fundamental relations for 2D multilayered composite structures

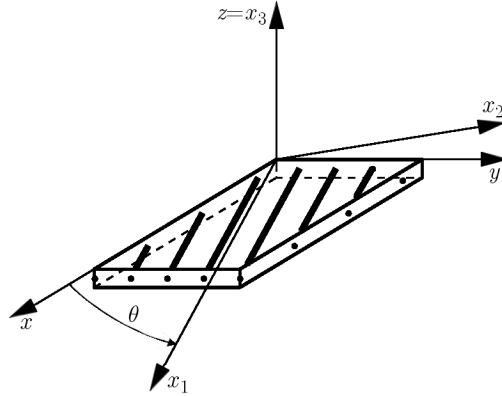


Fig. 1. Global and local coordinate systems ( $x_1 \equiv x'$ ,  $y_1 \equiv y$ ,  $z \equiv z'$ )

Usually thin plies in the laminate (Fig. 1) can be considered to be under a plane stress with all the stress components in the out-of-plane direction  $z$  being approximately zero. In the 3D case the generalized Hooke law (the local coordinate system  $x_1x_2z$  associated with fibres) is reduced to

$$\sigma'_i(x_1, x_2, z) = C'_{ij}\varepsilon'_j(x_1, x_2, z) \quad i, j = 1, 2, 6 \quad (2.1)$$

where

$$\begin{aligned} C'_{11} = Q_{11} &= \frac{E_1}{1 - \nu_{12}\nu_{21}} & C'_{12} = Q_{12} &= \frac{\nu_{12}E_2}{1 - \nu_{12}\nu_{21}} \\ C'_{22} = Q_{22} &= \frac{E_2}{1 - \nu_{12}\nu_{21}} & C'_{66} = Q_{66} &= G_{12} \end{aligned}$$

and  $\sigma'$  denotes the tensor of in-plane stress components, and  $\varepsilon'$  the tensor of in-plane strain components. Let us consider that the ply material axes are rotated by an angle  $\theta$  with respect to the global reference system  $(xyz)$  – Fig. 1. In the global system, writing the Hooke law

$$\sigma_i(x, y, z) = C_{ij}\varepsilon_j(x, y, z) \quad i, j = 1, 2, 6 \quad (2.2)$$

and using the Tsai-Pagano invariant formulation, all components of the stiffness matrix  $\mathbf{C}$  can be written in the invariant form

$$\begin{aligned} C_{11} &= U_1 + U_2 \cos 2\theta + U_3 \cos 4\theta & C_{12} &= U_4 - U_3 \cos 4\theta \\ C_{22} &= U_1 - U_2 \cos 2\theta + U_3 \cos 4\theta & C_{16} &= \frac{1}{2}U_2 \sin 2\theta + U_3 \sin 4\theta \\ C_{26} &= \frac{1}{2}U_2 \sin 2\theta - U_3 \sin 4\theta & C_{66} &= U_5 - U_3 \cos 4\theta \end{aligned} \quad (2.3)$$

where

$$\begin{aligned} U_1 &= \frac{1}{8}(3Q_{11} + 3Q_{22} + 2Q_{12} + 4Q_{66}) & U_2 &= \frac{1}{2}(Q_{11} - Q_{22}) \\ U_3 &= \frac{1}{8}(Q_{11} + Q_{22} - 2Q_{12} - 4Q_{66}) & U_4 &= \frac{1}{8}(Q_{11} + Q_{22} + 6Q_{12} - 4Q_{66}) \\ U_5 &= \frac{1}{2}(U_1 - U_4) \end{aligned}$$

The above relations are developed for a single ply (lamina). The laminate can be built of  $N$  layers, see Fig. 2, so that the stresses in the  $l$ -th ply are related to the strains in the following way

$$\sigma_i^{(l)}(x, y, z) = C_{ij}^{(l)} \varepsilon_j(x, y, z) \quad i, j = 1, 2, 6 \quad l = 1, 2, \dots, N \quad (2.4)$$

assuming that all ply strains are equal to the laminate strains. The stiffness matrix coefficients  $C_{ij}^{(l)}$  are defined with the use of Eq. (2.3) where the fibre orientations  $\theta$  are replaced by the symbol  $\theta_l$  referring to the fibre orientations of the  $l$ -th layer. From the assumption that the strains vary linearly through the laminate thickness, i.e.  $\varepsilon_i(x, y, z) = \varepsilon_i^0(x, y) + z\kappa_i(x, y)$  ( $i = 1, 2, 6$ ) one can find that relation (2.4) can be rewritten in the following form

$$\begin{aligned} N_i(x, y) &= A_{ij}\varepsilon_i^0(x, y) + B_{ij}\kappa_i(x, y) \\ M_i(x, y) &= B_{ij}\varepsilon_i^0(x, y) + D_{ij}\kappa_i(x, y) \end{aligned} \quad i, j = 1, 2, 6 \quad (2.5)$$

where the in-plane stress resultants  $N_i(x, y)$  and the stress couples  $M_i(x, y)$  are expressed as

$$\begin{aligned} N_i(x, y) &= \int_{-t/2}^{t/2} \sigma_i^{(l)} dz = \sum_{l=1}^N \sigma_i^{(l)} (z_l - z_{l-1}) \\ M_i(x, y) &= \int_{-t/2}^{t/2} \sigma_i^{(l)} z dz = \frac{1}{2} \sum_{l=1}^N \sigma_i^{(l)} (z_l^2 - z_{l-1}^2) \end{aligned} \quad i = 1, 2, 6 \quad l = 1, \dots, N \quad (2.6)$$

where  $\mathbf{A}$ ,  $\mathbf{B}$ ,  $\mathbf{D}$  are the extensional, coupling and bending stiffnesses, respectively, defined as follows

$$\begin{aligned} A_{ij} &= \sum_{l=1}^N C_{ij}^{(l)} (z_l - z_{l-1}) & B_{ij} &= \frac{1}{2} \sum_{l=1}^N C_{ij}^{(l)} (z_l^2 - z_{l-1}^2) \\ D_{ij} &= \frac{1}{3} \sum_{l=1}^N C_{ij}^{(l)} (z_l^3 - z_{l-1}^3) \end{aligned} \quad i, j = 1, 2, 6 \quad (2.7)$$

where  $z_l$  and  $z_{l-1}$  are the location coordinates of the top and the bottom surface of the lamina  $l$ .  $\varepsilon_i^0(x, y)$  are the components of the in-plane (membrane) strains, and  $\kappa_i(x, y)$  are the components of the vector of curvature ( $i = 1, 2, 6$ ).

### 3. Definition of design variables

In the 2D approach, topological variables defining the connectivity of particular structural elements in the structure (in the paper it denotes the stacking sequence of the individual layers in the laminate) are understood in the sense of the sequence of layers having prescribed discrete fibre orientations  $\theta_l$  in each individual ply. Commonly, it is assumed that the thicknesses of individual plies are identical, i.e.  $t_l = t/N$  – see Fig. 2. In order to assure great flexibility and generality in the formulation of various optimisation problems, different types of the above-mentioned discrete design variables must be represented in a similar unified manner, i.e. each design variable must be coded as a finite string of digits. Let us note that the angle-ply anti-symmetric laminates are considered only, however, it can be easily extended for an arbitrary laminate configuration. Using the classical method of coding, 1 represents  $0_2^\circ$ , 2 –  $\pm 45^\circ$ , 3 –  $90_2^\circ$ . Each design variable  $s$  representing the fibre orientation (i.e. 1, 2 and 3) is coded as a binary number and is called as a gene. The sequence  $\{1, 2, 1, 3\}$  is called a chromosome. Such a representation is not very convenient for optimisation problems since there is a lot of design variables

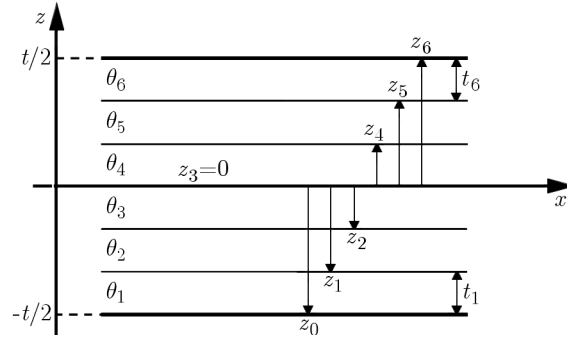


Fig. 2. Cross-section of the laminate ( $N = 6$ )

(increasing with the total number of plies  $N$ ) and, in addition, various stacking sequences are described by the identical values of the  $\mathbf{A}$ ,  $\mathbf{B}$ ,  $\mathbf{D}$  matrices. Therefore, we propose to adopt herein a special type of integer variables  $x_r^{\{A,D\}}$  ( $r = 1, 2, 3$ ) introduced by Muc (1997) that are completely different than those introduced by Miki (1986), Fukunaga and Vanderplaats (1991). The new design variables represent triangles in the design space, see Fig. 3. However, there is

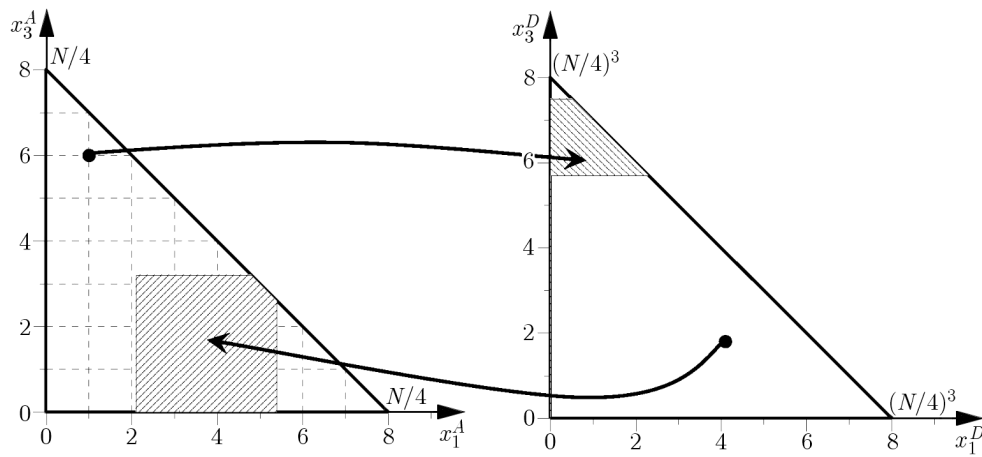


Fig. 3. Graphical representation of design variables

no unique mapping between the spaces  $x_r^A$  and  $x_r^D$ . For the assumed laminate configuration, the  $\mathbf{B}$  matrix is identically equal to zero, whereas the stiffnesses  $\mathbf{A}$  and  $\mathbf{D}$  can be written in the following way

$$\begin{aligned}
 A_{11} &= t(U_1 - U_3) + \frac{4t}{N}U_2(x_1^A - x_3^A) + \frac{8t}{N}U_3(x_1^A + x_3^A) \\
 A_{12} &= t(U_4 + U_3) - \frac{8t}{N}U_3(x_1^A + x_3^A) \\
 A_{22} &= t(U_1 - U_3) - \frac{4t}{N}U_2(x_1^A - x_3^A) + \frac{8t}{N}U_3(x_1^A + x_3^A) \\
 A_{66} &= t(U_5 + U_3) - \frac{8t}{N}U_3(x_1^A + x_3^A)
 \end{aligned} \tag{3.1}$$

and

$$D_{11} = \frac{t^3}{12}(U_1 - U_3) + \frac{1}{12}\left(\frac{4t}{N}\right)^3 U_2(x_1^D - x_3^D) + \frac{1}{6}\left(\frac{4t}{N}\right)^3 U_3(x_1^D + x_3^D)$$

$$\begin{aligned}
D_{12} &= \frac{t^3}{12}(U_4 + U_3) - \frac{1}{6}\left(\frac{4t}{N}\right)^3 U_3(x_1^D + x_3^D) \\
D_{22} &= \frac{t^3}{12}(U_1 - U_3) - \frac{1}{12}\left(\frac{4t}{N}\right)^3 U_2(x_1^D - x_3^D) + \frac{1}{6}\left(\frac{4t}{N}\right)^3 U_3(x_1^D + x_3^D) \\
D_{66} &= \frac{t^3}{12}(U_5 + U_3) - \frac{1}{6}\left(\frac{4t}{N}\right)^3 U_3(x_1^D + x_3^D)
\end{aligned} \tag{3.2}$$

where

$$\begin{aligned}
x_r^{\{A,D\}} &= \sum_{k=1}^{N/4} \{1, [3k(k-1) + 1]\} \cos(2\theta) \Xi(\alpha_r) \\
\Xi(\alpha_r) &= \begin{cases} 1 & \text{where } \alpha_r = \theta \\ 0 & \text{where } \alpha_r \neq \theta \end{cases} \\
\alpha_r &= 90^\circ \frac{r-1}{2} \quad r = 1, 2, 3
\end{aligned} \tag{3.3}$$

Let us note that using the above notation all terms in the stiffness matrix are uniquely represented by the set of four integer variables  $\{x_1^A, x_3^A, x_1^D, x_3^D\}$ . The terms having the index  $r = 2$  are identically equal to 0 since they correspond to the plies having fibres oriented at  $45^\circ$ . The integer numbers  $x_1^A, x_3^A$  represent directly the number of plies with fibres oriented at  $0^\circ$  and  $90^\circ$ , respectively, since the following relation is always fulfilled

$$x_1^A + x_3^A + x_2^A = \frac{N}{4} \tag{3.4}$$

where  $x_2^A = N_{45}/4$ , and  $N_{45}$  denotes the total number of plies oriented at  $45^\circ$ . With the aid of Eqs. (3.1)-(3.4) it is possible to define feasible regions for our new design variables – the triangles presented in Fig. 3. Two sets of variables  $\{x_1^A, x_3^A\}$  and  $\{x_1^D, x_3^D\}$  are not independent, however, using their definition (Eq. (3.3)) it is possible to evaluate the ranges of their variations demonstrated in Fig. 3 in the form of quadrilaterals

$$\begin{aligned}
(x_1^A)^3 &= \sum_{k=1}^{x_1^A} [3k(k-1) + 1] \leq x_1^D \leq \sum_{k=N/4+1-x_1^A}^{N/4} [3k(k-1) + 1] = \left(\frac{N}{4}\right)^3 - \left(\frac{N}{4} - x_1^A\right)^3 \\
(x_3^A)^3 &= \sum_{k=1}^{x_3^A} [3k(k-1) + 1] \leq x_3^D \leq \sum_{k=N/4+1-x_3^A}^{N/4} [3k(k-1) + 1] = \left(\frac{N}{4}\right)^3 - \left(\frac{N}{4} - x_3^A\right)^3 \\
x_1^D + x_3^D &\leq \left(\frac{N}{4}\right)^3
\end{aligned} \tag{3.5}$$

Knowing the values of the  $\{x_1^D, x_3^D\}$  variables, one can derive from relations (3.1), (3.2) the upper and lower bounds of the  $\{x_1^A, x_3^A\}$  variables that have to be integer numbers belonging to the triangular domain shown in Fig. 3. However, in the optimisation procedure they are treated as continuous variables since they are always normalised (by the division of them by  $N/4$  and  $(N/4)^3$ , respectively) and they belong to the interval  $[0, 1]$ . The normalised variables are denoted by the bar over the symbols, i.e. as  $\{\bar{x}_1^A, \bar{x}_3^A\}$ ,  $\{\bar{x}_1^D, \bar{x}_3^D\}$ . The optimal solutions are completely independent of the total number of plies  $N$  and, in addition, the definition of the appropriate terms in the stiffness matrices  $\mathbf{A}$  and  $\mathbf{D}$  has an identical form, although they are functions of different variables. Such a definition may be also very useful for the pseudorandom generation of the design variables.

If the optimal solutions are found (in the sense of four variables  $\{\bar{x}_1^A, \bar{x}_3^A\}$ ,  $\{\bar{x}_1^D, \bar{x}_3^D\}$ ) the decoding procedure is required to represent the above-mentioned variables by the appropriate

stacking sequences. The decoding procedure can be easily conducted with the use of the symbolic package Mathematica. The fundamental two operations are given below

```
a = Table[3 * l * (l - 1) + 1, l, N/4];
f = Subsets[a, L];
```

First of all, a list of values of the expression “ $3l(l - 1) + 1$ ” is generated when the natural number  $l$  runs from 1 to  $N/4$  – see Eq. (2.3). Assuming  $N = 16$ , table “a” takes the form:  $\{1, 7, 19, 37\}$ . Then a finite number of subsets “f” having exactly “L” elements is constructed from the list “a”. For instance, for  $L = 2$  the subsets “f” are following:  $\{1, 7\}$ ,  $\{1, 19\}$ ,  $\{1, 37\}$ ,  $\{7, 19\}$ ,  $\{7, 37\}$ ,  $\{19, 37\}$ . If  $L = 2$  defines the number of plies oriented at  $0^\circ$  (i.e.  $x_1^A = 2$ ) then each of the subsets represents the laminates (in fact the upper part of the laminate where the symbol  $0^\circ$  corresponds to the pair of plies having the  $0^\circ$  orientation):  $[0^\circ, 0^\circ, \div, \div]$ ,  $[0^\circ, \div, 0^\circ, \div]$ ,  $[0^\circ, \div, \div, 0^\circ]$ ,  $[\div, 0^\circ, 0^\circ, \div]$ ,  $[\div, 0^\circ, \div, 0^\circ]$ ,  $[\div, \div, 0^\circ, 0^\circ]$ . According to definition (3.3), all laminates have the same value  $x_1^A = 2$  but different values of  $x_1^D$  equal to: 8, 20, 38, 26, 44, 56, respectively. In addition, the first laminate can be characterized by two different values of  $x_3^D$ , i.e.:  $[0^\circ, 0^\circ, 45^\circ, 90^\circ] - x_3^D = 37$  or  $[0^\circ, 0^\circ, 90^\circ, 45^\circ] - x_3^D = 19$ . In both cases,  $x_2^A = x_3^A = 1$ . The example demonstrates evidently the non-uniqueness of the mapping presented in Fig. 3. However, as four design variables are known (e.g.  $x_1^A = 2$ ,  $x_3^A = 1$  and  $x_1^D = 8$ ,  $x_3^D = 19$ ) the lamination sequence can be derived uniquely – it corresponds to  $[0^\circ, 0^\circ, 90^\circ, 45^\circ]$ . Therefore, to decode the lamination sequence from the set of the normalized design variables  $\{\bar{x}_1^A, \bar{x}_3^A\}$ ,  $\{\bar{x}_1^D, \bar{x}_3^D\}$ , it is necessary to conduct the following operations: Step 1) to round the values  $\{\bar{x}_1^A * (N/4), \bar{x}_3^A * (N/4)\}$  to the nearest integers, Step 2) to find the subsets “f” corresponding to  $\bar{x}_1^A \approx \bar{x}_1^A * (N/4)$ , compute the sum of each of the elements in the subsets “f” and find the nearest integer to the real number  $\bar{x}_1^D * (N/4)^3$ , Step 3) to repeat step 2 for the value  $\bar{x}_3^A \approx \bar{x}_3^A * (N/4)$ , creating new subsets for the layers oriented at  $90^\circ$ , but selecting empty spaces only (noted as  $\div$  in the laminate in the above example), Step 4) to fill the rest of empty spaces in the laminate by the layers oriented at  $45^\circ$ . To verify the convergence, it is possible to increase the total number of layers  $N$ .

The decoding procedure is simple using symbolic packages. In many cases (one of them will be discussed further), the optimal design is not represented by all design variables, and the decoding method has to be slightly modified.

#### 4. Buckling and the First-Ply-Failure of plates

Many experimental results on the buckling of composite material plates have been presented over the last years. They are summarized in Muc (1988), Muc and Gurba (2001). In general, they tend to indicate that the theory for composites is rather in good agreement with experiments. The experiments demonstrate evidently that for thin-walled flat composite plates, the loss of stability is not equivalent to the catastrophic failure of structures. The catastrophic failure in form of the limit carrying capacity may occur for thicker plates and it is associated with the First-Ply-Failure (FPF). For plates with a cutout, delaminations or stiffened, the failure mode may be in form of bifurcation buckling, but the final damage is usually associated with other modes of failure. For flat plates, the comparison between experimental and theoretical results is conducted with the use of linear prebuckling theory according to experimental observations. For more complicated plated structures, the nonlinear prebuckling and postbuckling analysis is required since the final failure mode is associated, e.g., with local buckling modes or failure of a core for sandwiches. Therefore, for flat bi-axially compressed rectangular plates, it is assumed that a critical multiplier of loading corresponding to the global loss of stability  $\lambda_b$  can be expressed in the following form

$$\lambda_b(s) = \frac{(m\pi/a)^2}{P_x(1+k\beta_m^2)} [D_{11} + (D_{12} + 2D_{66})\beta_m^2 + D_{22}\beta_m^4] \quad \beta_m = \frac{na}{mb} \quad k = \frac{P_y}{P_x} \quad (4.1)$$

where  $a, b$  are geometrical plate dimensions, and  $m, n$  are numbers of half-waves in two perpendicular directions corresponding to the plate co-ordinate system, and  $P_x$  is the axial compressive force in the  $x$  direction.  $s$  denotes the vector of design variables having 2 independent normalized real variables  $\{\bar{x}_r^A, \bar{x}_r^D\}$  defined in the interval  $[0, 1]$  representing 3 different fibre orientations and various stacking sequences in the laminate. Using the notation introduced in Eq. (4.1), the critical multiplier of loading can be written as follows

$$\lambda_b = \Omega_m(Z_1 + Z_2\bar{x}_1^D + Z_3\bar{x}_3^D) \quad (4.2)$$

where

$$\begin{aligned} \bar{x}_r^D &= \left(\frac{4}{N}\right)^3 x_r^D & \Omega_m &= \frac{(n\pi/b)^2 t^3}{P_x(1+k\beta_m^2)\beta_m^2 12} \\ Z_1 &= U_1(1 + \beta_m^2)^2 + U_3(6\beta_m^2 - 1 - \beta_m^4) & Z_2 &= U_2(1 - \beta_m^4) + 2U_3(1 - 6\beta_m^2 + \beta_m^4) \\ Z_3 &= 2U_3(1 - 6\beta_m^2 + \beta_m^4) - U_2(1 - \beta_m^4) & r &= 1, 2, 3 \end{aligned}$$

It is also worth to point out also that the validity of relation (4.1) is strictly limited by the values of  $t/[\text{Min}(a, b)]$  ratio. For the ratio higher than 0.05, it is necessary to include transverse shear effects employing, for instance, the Mindlin hypothesis.

It is well-known that buckling loads (4.2) are straight lines in the convex design space (Fig. 3). Since for the known composite materials  $U_1$  is always greater than  $U_3$ , the coefficient  $Z_1$  is always positive, whereas  $Z_2$  and  $Z_3$  may be positive, equal to zero or negative. According to the classical theory of mathematics for the prescribed mode of buckling (i.e.  $m$  and  $n$ ) in the feasible domain of design variables  $x_1^D, x_3^D$ , the maximal value of the parameter  $\lambda_b$  defined by Eq. (4.2) may exist at the vertices of the triangle (points  $A, B, C$  – unimodal solutions) or along the lines  $AB$  and  $BC$  (e.g. points  $D$  and  $E$ , bimodal solutions – degenerated solutions since one of the variables  $x_1^D$  or  $x_3^D$  is equal to zero) – Fig. 4.

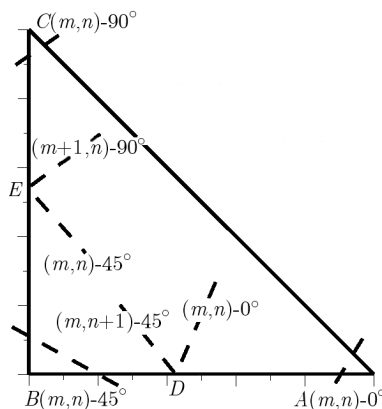


Fig. 4. Positions of the optimal buckling loads for three discrete fibre orientations

4.1. Unimodal solutions

The variations of the coefficients  $Z_1, Z_2$  and  $Z_3$  with the geometrical ratios  $a/b$  are demonstrated in Fig. 5. Their values correspond directly to the location of optimal fibre orientations with respect to the  $a/b$  ratio, i.e.  $\bar{x}_1^D = 1, \bar{x}_3^D = 0$  – orientation  $0^\circ$ ;  $\bar{x}_1^D = 0, \bar{x}_3^D = 0$  – orientation  $45^\circ$ ;  $\bar{x}_1^D = 0, \bar{x}_3^D = 1$  – orientation  $90^\circ$ .

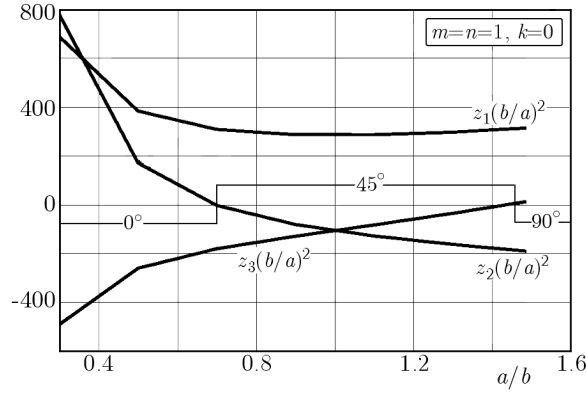


Fig. 5. Variations of the coefficients in Eq. (4.2)

With the use of the introduced design variables, the analytical unimodal optima can also be easily derived. They can be written in the following way:

— equivalent to the point  $A$ ,  $Z_2 > 0$  and  $Z_3 < 0$

$$x_1^D = \left(\frac{N}{4}\right)^3 \quad x_3^D = 0 \quad \text{if} \quad \beta_m \leq \sqrt{\frac{-3\varphi + \sqrt{8\varphi^2 + 1}}{1 - \varphi}} \quad (4.3)$$

— equivalent to the point  $B$ ,  $Z_2 < 0$  and  $Z_3 < 0$

$$x_1^D = 0 \quad x_3^D = 0 \quad \text{if} \quad \sqrt{\frac{-3\varphi + \sqrt{8\varphi^2 + 1}}{1 - \varphi}} \leq \beta_m \leq \sqrt{\frac{3\varphi + \sqrt{8\varphi^2 + 1}}{1 - \varphi}} \quad (4.4)$$

— equivalent to the point  $C$ ,  $Z_2 < 0$  and  $Z_3 > 0$

$$x_1^D = 0 \quad x_3^D = \left(\frac{N}{4}\right)^3 \quad \text{if} \quad \beta_m \geq \sqrt{\frac{3\varphi + \sqrt{8\varphi^2 + 1}}{1 + \varphi}} \quad (4.5)$$

where  $\varphi = 2U_3/U_2$ .

In the above relations, the estimations are computed from the equalities:

— equivalent to  $Z_1 = 0$

$$\lambda_b \left[ x_1^D = \left(\frac{N}{4}\right)^3, x_3^D = 0, m, n \right] = \lambda_b \left[ x_1^D = 0, x_3^D = 0, m, n \right] \quad (4.6)$$

— equivalent to  $Z_3 = 0$

$$\lambda_b \left[ x_1^D = 0, x_3^D = 0, m, n \right] = \lambda_b \left[ x_1^D = 0, x_3^D = \left(\frac{N}{4}\right)^3, m, n \right] \quad (4.7)$$

where the first relation describes the equality of buckling loads for the laminates oriented at  $0^\circ$  and  $45^\circ$ , and the second, the equality of buckling loads for the laminates oriented at  $45^\circ$  and  $90^\circ$ .

#### 4.2. Bimodal solutions

The bimodal solutions correspond to situations as the buckling load is identical for two neighbouring buckling modes (e.g.  $m$  and  $m + 1$ ) – see also Muc (1988) (continuous angle-ply orientations). Let us note that the identical procedure is conducted in the buckling analysis of isotropic structures although the solutions are not called the bimodal ones. For isotropic plates constructing the classical “chain curve” for buckling loads versus the  $a/b$  ratio for different wave numbers  $m$ , it is possible to find such values of the  $a/b$  ratio that correspond to two neighbouring

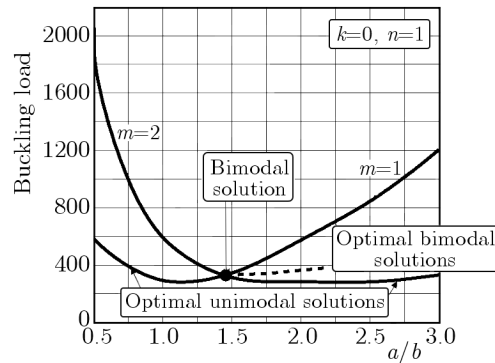


Fig. 6. Optimal unimodal and bimodal solutions

buckling modes  $m$  and  $m + 1$  (e.g. for uniaxially compressed plates:  $a/b = \sqrt{2}$  as  $m = 1$  and 2,  $a/b = \sqrt{6}$  as  $m = 2$  and 3 etc.). Figure 6 shows a part of the chain curve for laminated plates as well as the optimal unimodal solutions – the lower bound envelope of buckling loads for different values of  $m$ . The dot represents the classical bimodal solutions.

For laminated plates, the critical multiplier  $\lambda_b$  (Eqs. (4.1) or (4.2)) is not only a function of the geometrical  $a/b$  ratio but also of the design variables  $s$ . Therefore, for the identical  $a/b$  ratio, there may exist a finite number (discrete variables) of bimodal solutions. Some of them may correspond to the higher values of buckling loads than for unimodal solutions. They will be called the optimal bimodal solutions (Fig. 6).

The bimodal solution presented as the dot in Fig. 6 demonstrates that the unimodal optimal solutions exist for two different modes of buckling  $m = 2$  and  $m = 1$ , however, each of them corresponds to different fibre orientations ( $\pm 45^\circ$  and  $90^\circ$ , respectively). For uniaxial compression ( $k = 0$ ), the maximal buckling load occurs always for plies having fibres oriented at  $\alpha_2 = \pm 45^\circ$ . For each buckling mode (considering separately the modes  $m = 1$  and  $m = 2$ ), the buckling load at the vertex  $B$  is higher than at the vertices  $A$  and  $C$ , and it takes a lower value (for  $m = 1$  and  $a/b < 1.445$ ) than the corresponding buckling load at the vertex  $B$  for  $m = 2$  – see Eq. (4.4). If  $a/b = 1.445$ , the optimal unimodal fibre orientations switch from  $\pm 45^\circ$  to  $90^\circ$  for  $m = 1$ . However, the latter case does not satisfy the buckling criterion – it is not the lower bound with respect to buckling modes since unimodal buckling loads for plies having the orientation  $90^\circ$  have lower values for  $m = 2$  than those for the lower buckling mode ( $m = 1$ ). Of course, the unimodal solutions for  $\pm 45^\circ$  and  $m = 2$  cannot be treated as optimal ones because this orientation gives lower buckling loads for  $m = 1$ . Thus, the bimodal constraint becomes active.

For discrete design variables, it is possible to find two potential candidates for the optimum considering each wave numbers of buckling, i.e.  $(m, n)$  and  $(m + 1, n)$ . Such type of optimal solutions is represented by the points  $D$  and  $E$  in Fig. 4. The identical analysis can be carried out in the similar manner for the  $(m, n)$  and  $(m, n + 1)$  buckling modes. Of course, the points  $D$  and  $E$  are not single candidates for the bimodal solutions. The equalisation of the buckling load coefficients (Eq. (4.1)) for the neighbouring buckling modes (i.e.  $m, n$  and  $m + 1, n$ ) leads to a finite number of solutions represented by a straight line in the design space  $(x_1^D, x_3^D)$ . Using Eqs. (4.6) and (4.7), the bimodal solutions can be found at the boundaries of the triangle only since those values offer the highest buckling load among them. The proof of this conclusion is a trivial one since for each buckling mode the straight lines described by Eq. (4.1) create a family of parallel lines (parametrized by the value of buckling load) whose maximum occurs at the opposite vertices of the triangle – one vertex where the maximum occurs at the point  $B$  for the mode  $(m + 1, n)$ , and the second maximum located at the point  $C$  for the mode  $(m, n)$ .

The bimodal solutions can be found analytically from the following relations

$$\begin{aligned}\bar{x}_1^D &= 0 \\ \lambda_b(m, n) &= \Omega_m [Z_1(m) - \bar{x}_3^D U_2(1 - \beta_m^4) + 2\bar{x}_3^D U_3(1 - 6\beta_m^2 + \beta_m^4)] \\ &= \lambda_b(m + 1, n) = \Omega_{m+1} Z_1(m + 1)\end{aligned}\quad (4.8)$$

The relations are valid for  $a/b > 0.7$ . In the opposite case, the bimodal solutions are located along the line  $\bar{x}_3^D = 0$ .

### 4.3. FPF constraints

For the assumed laminate configuration and considering the membrane state only in the global coordinate system, the strain tensor is reduced to two nonzero components written in the following way (see Eq. (2.5)):

$$\varepsilon_1^0 = \frac{\lambda_{FPF} P_x (A_{22} - kA_{12})}{A_{11}A_{22} - A_{12}^2} \quad \varepsilon_2^0 = \frac{\lambda_{FPF} P_x (kA_{11} - A_{12})}{A_{11}A_{22} - A_{12}^2} \quad \varepsilon_6^0 = 0 \quad (4.9)$$

The strains in the local coordinate system of the ply having the orientation  $\alpha_r$  take the following form

$$\varepsilon'_1 = \varepsilon_1^0 \cos^2 \alpha_r + \varepsilon_2^0 \sin^2 \alpha_r \quad \varepsilon'_2 = \varepsilon_1^0 \sin^2 \alpha_r + \varepsilon_2^0 \cos^2 \alpha_r \quad \varepsilon'_6 = (\varepsilon_2^0 - \varepsilon_1^0) \sin 2\alpha_r \quad (4.10)$$

For each individual ply, the above mentioned local strains are compared with the allowable strains along the fibres  $\varepsilon_{1allowable}^{local}$ , in the direction perpendicular to the fibres  $\varepsilon_{2allowable}^{local}$  and with the shear strains  $\gamma_{12allowable}^{local}$ , respectively. Thus, for each discrete fibre orientation  $\alpha_r$  we have three inequality FPF constraints. However, one can easily find that each FPF relation may be presented in the identical form

$$\begin{aligned}2t(U_1 + U_4)(tQ_{66} + F_2^A) - (F_1^A)^2 &= \lambda_{FPF} P_x (p_1 + p_2 F_1^A + p_3 F_2^A) \frac{1}{\varepsilon_{allowable}^{local}} \\ F_1^A &= \frac{4t}{N} U_2 \sum_{r=1}^{r_{max}+1} x_r^A \cos(2\alpha_r) \quad F_2^A = \frac{8t}{N} U_3 \sum_{r=1}^{r_{max}+1} x_r^A \cos^2(2\alpha_r)\end{aligned}\quad (4.11)$$

where  $\varepsilon_{allowable}^{local}$  denotes the appropriate allowable strains for the plies, and  $p_i$  ( $i = 1, 2, 3$ ) are appropriate constants derived from equations (4.9) and (4.10). The curves described by Eq. (4.11) represent ellipses in the design space  $\{x_1^A, x_3^A\}$ . It is obvious that with the aid of any of numerical packages (Mathematica, Maple, Matlab, Mathcad) it is possible to compute values of  $\lambda_{FPF}$  (Eq.14) for all values of  $x_1^A, x_3^A$  as well as the prescribed mechanical and geometrical properties of the plate and the loading parameter  $k$ . Such a procedure can be easily conducted for all components of strains, assuming different allowable values for tension and compression. Finally, the results are collected in a table (called as FPFTable) that is parametrized by the values of  $x_1^A, x_3^A$  and the failure mode (Eq. (4.11)).

## 5. Optimization problem

The optimisation problem is formulated as follows

$$\max_s (\min_{m,n} \lambda_b) \quad (5.1)$$

where  $\lambda_b$  denotes a critical multiplier of loading corresponding to the global loss of stability and  $s$  denotes the set of design variables  $\{\bar{x}_1^D, \bar{x}_3^D\}$ .

The analysed problem may be subjected to various subsidiary constraints written in the following form:

— Bimodal constraints

$$\lambda_b[m, n] \leq \lambda_b[m + 1, n] \quad \text{and} \quad \lambda_b[m, n] \leq \lambda_b[m, n + 1] \quad (5.2)$$

— FPF constraints

$$\lambda_{FPF} \leq \lambda_b \quad (5.3)$$

Constraint (5.2) presents two conditions for each wave number in buckling independently, and the values of buckling coefficients  $\lambda_b$  are derived from Eqs. (4.1) or (4.2).

The optimization analysis is carried out for the prescribed mechanical constants, the total number of layers  $N$ , the loading parameter  $k$  and the geometrical ratio  $a/b$ . At the beginning, the buckling loads are computed for all vertices of the triangle (Fig. 3); they correspond to the fibres oriented in all plies at  $0^\circ$ ,  $45^\circ$  and  $90^\circ$ , respectively. Those values are collected in a table (called as UNITable) and parametrized by the values  $m$  and  $n$  (selected in the prescribed range, let say from 1 to 5). Then, the optimization is divided into four procedures described below.

- I. *Unimodal optimum.* There are two integer numbers  $m$  and  $n$  such that for all vertices of the triangle, the values in the UNITable have the global minimum with respect to them. In addition, condition (3.5)<sub>1</sub> is satisfied (comparison with the values in the FPFTable). The optimal values can be computed from relations (4.3)-(4.5). The laminate stacking sequence is easily determined.
- II. *Bimodal optimum.* There are two integer numbers  $m$  and  $n$  such that for all vertices of the triangle the values in the UNITable have not the global minimum with respect to them, i.e. the bimodal constraints become active and if condition (5.2) is not satisfied (comparison with the values in the FPFTable) then the optimal normalised design variables  $\{\bar{x}_1^D, \bar{x}_3^D\}$  are computed from relations (4.8). It is necessary to decode the results to obtain the optimum in form of the laminate stacking sequence. To demonstrate it, let assume that the plate is made of  $N = 64$  layers,  $a/b = 0.5$  and is biaxially compressed, i.e.  $k = 2$ ,  $n = 1$ . The optimum occurs for  $x_1^D = 1963.307$ ,  $x_2^D = 3899.693$ ,  $x_3^D = 0$ . The domain of possible variations of the number “L” is created with the help of inequalities (3.5), and let it be equal to 7. For each generated subset “f”, the sum of the elements in the subset is computed in the loop and compared with the rounded to two natural numbers real values of the optimal solution (1963 or 1964). Having, for instance, the subset  $\{91, 127, 169, 217, 331, 397, 631\}$  (the sum is equal to 1963) it is possible to recognize immediately that from the whole laminate represented by the table “a” ( $N/4 = 16$ ) the elements having the nonzero values in the whole table, i.e.  $\{\div, \div, \div, \div, \div, 91, 127, 169, 217, \div, 331, 397, \div, \div, 631, \div\}$  are replaced by the pairs oriented at  $0^\circ$ , whereas the symbol “ $\div$ ” by the pairs oriented at  $\pm 45^\circ$ . It is worth to add that it is possible to find other 35 laminate configurations (subsets “f”) that give the same sum 1963. There is multiplicity of the solutions since the optimum is represented by two variables only.
- III. *Bimodal and FPF optimum.* Similarly as in the previous case II, the bimodal optimum becomes active, however, the FPF load is lower than the optimum bimodal solution (condition (5.3) is satisfied) and the optimum exists inside the triangles plotted in Fig. 3. The optimum can be found from the relation

$$\lambda_b[m, n] = \lambda_b[m + 1, n] = \lambda_{FPF} \quad (5.4)$$

Using the appropriate relation for  $\lambda_b$  (4.2) and  $\lambda_{FPF}$  (4.9), it is possible to express the above equality constraint conditions in the following form:  $\bar{x}_1^D = p(\bar{x}_1^A, \bar{x}_3^A)$ ,  $\bar{x}_3^D = q(\bar{x}_1^A, \bar{x}_3^A)$  where  $p$  and  $q$  are analytical algebraic functions. Inserting those results to the definition of buckling loads (4.2), it is possible to find the maximal buckling load with respect to the values  $\bar{x}_1^A, \bar{x}_3^A$  searching for the maximum by building the table for all possible variations of the values  $x_1^A, x_3^A$   $((N/4)[(N/4) - 3] + 2$  possible values inside the half of the triangles) or using the Mathematica procedure “Maximize”. For the optimal values of  $x_1^A, x_3^A$  design variables, it is possible to derive the optimal values of  $\bar{x}_1^D, \bar{x}_3^D$  and find the optimal stacking sequences with the aid of the decoding procedure presented in Section 3. The discussed problem of both FPF and bimodal active constraints occurs, e.g. for plates:  $a/b = 4$ ,  $k = 0.25$ .

**IV. FPF optimum.** If the FPF is the dominant failure mode (thick plates), the optimum can be found directly from relation (4.9) searching for the maximum similarity as in the previous case. Since the optimum is a function of the membrane parameters, one can observe again the multiplicity of optimal laminate configurations.

## 6. Concluding remarks and further works

In the paper, the proposal of a new discrete design variables that are used in the buckling and FPF optimisation problems is shown. It is demonstrated that in the buckling and FPF analysis of plates, four types of solutions may exist, i.e.:

- Unimodal buckling solutions – unique determination of optimal stacking sequences.
- Bimodal buckling solutions – multiplicity of optimal stacking sequences (bending state only).
- FPF and bimodal buckling solutions – unique determination of optimal stacking sequences (flexural and membrane design variables).
- FPF – multiplicity of optimal stacking sequences (membrane state only).

In our opinion, the new set of design variables demonstrates a lot of the advantages in comparison with the existing ones, i.e.:

- It allows us to derive unique analytical solutions.
- It explains the uniqueness and multiplicity of possible laminate configurations being a representation of laminate discrete configurations.
- It shows a simple symbolic method for the derivation of multiple optimal configurations from the used set of discrete design variables (the so-called decoding method).

The analysed example (buckling and FPF of bi-axially compressed plates) is relatively simple since the optimisation problem is characterized by flexural and membrane properties only, given by analytical formulae. The next step is connected with simultaneous application of the proposed design variables to optimisation problems characterised by analytical solutions that include both bending, membrane and coupling effects. Finally, we intend to include the proposed methodology into numerical FE codes in the similar manner as described by Muc and Gurba (2001).

### Acknowledgement

The National Science Center (Poland) UMO-2013/09/B/ST8/00178 is gratefully acknowledged for the financial support.

### References

1. FUKUNAGA H., VANDERPLAATS G.N., 1991, Stiffness optimization of orthotropic laminated composites using lamination parameters, *AIAA Journal*, **29**, 641-648
2. GROSSET L., LERICHE R., HAFTKA R., 2006, A double-distribution statistical algorithm for composite laminate optimization, *Structural and Multidisciplinary Optimization*, **31**, 49-59
3. IEEE Neural Network Council, Glossary of Evolutionary Computation terms, Standing Committee on Standards, IEEE, Piscatway, NY, 1996
4. KAUFFMAN S.A., 1993, *The Origins of Order: Self-Organization and Selection in Evolution*, Oxford University Press, New York
5. MIKI M., 1986, Optimum design of fibrous laminated plates subjected to axial compression, *Proceedings of 3rd Japan-US Composite Materials Conference*, Tokyo, 673-81
6. MUC A., 1988, Optimal fibre orientations for simply -supported plates under compression, *Composite Structures*, **9**, 161-172
7. MUC A., 1997, A new set of design variables in stacking sequence optimization under buckling and strength constraints, *Proceedings of WCSMO-2*, **2**, 693-698
8. MUC A., GURBA W., 2001, Genetic algorithms and finite element analysis in optimization of composite structures, *Composite Structures*, **54**, 275-281
9. MUC A., MUC-WIERZGOŃ M., 2012. An evolution strategy in structural optimization problems for plates and shells, *Composite Structures*, **94**, 1461-1470

*Manuscript received May 17, 2015; accepted for print August 13, 2015*